Tropical tropospheric ozone columns from nadir retrievals of GOME-1/ERS-2, SCIAMACHY/Envisat, and GOME-2/MetOp-A (1996-2012)

Elpida Leventidou[1], Kai-Uwe Eichmann[1], Mark Weber[1], and John P. Burrows[1]

[1]Institute of Environmental Physics (IUP), University of Bremen, Bremen, Germany

Correspondence to: E. Leventidou (levent@iup.physik.uni-bremen.de)

Abstract. Tropical tropospheric ozone columns are retrieved with the Convective Clouds Differential (CCD) technique using total ozone columns and cloud parameters from different European satellite instruments. Monthly mean tropospheric column amounts [DU] are calculated by subtracting the above cloud ozone column from the total column. A CCD algorithm (CCD_IUP) has been

5   developed (as part of the verification algorithm development for TROPOMI on Sentinel 5-precursor mission) which was applied to GOME/ ERS-2 (1995-2003), SCIAMACHY/ Envisat (2002-2012), and GOME-2/ MetOpA (2007-2012) measurements. Thus a unique long-term record of monthly mean tropical tropospheric ozone columns (20°S–20°N) from 1996 to 2012 is now available. An extensive error analysis has been performed, estimating the tropospheric ozone column uncertainties

10   being between 5 and 7 DU (25–36%). Validation with SHADOZ ozonesonde data show that tropospheric ozone columns from CCD and collocated integrated ozonesonde profiles from the surface up to 200 hPa are in good agreement with respect to range, inter-annual variations, and variances. Biases within ±5 DU and RMS errors of less than 10 DU are found. CCD comparisons using SCIAMACHY data with tropospheric ozone columns derived from Limb Nadir Matching have shown that

15   CCD results are less noisy and correlate better with ozonesondes. The 17-year dataset can be helpful for evaluating chemistry models and performing climate change studies.

1 Introduction

Stratospheric ozone is well known for protecting the surface from harmful ultraviolet solar radiation. However, ozone in the troposphere plays a more complex role. Although a small amount of

20   ozone of about 500 Tg/yr (IPCC, 2007) enters the troposphere either by stratospheric intrusions at midlatitudes or by wave breaking in the subtropics, tropospheric ozone levels cannot be explained by the stratosphere-troposphere exchange (STE) processes alone (Crutzen, 1995; Jacob, 2000). Unlike other greenhouse gases, ozone is a secondary pollutant produced exclusively in the atmosphere. It is mainly generated from the photochemical oxidation with 3420±770 Tg/yr (IPCC, 2007) of

25   three major precursors: carbon monoxide (CO), methane (CH_4) and non-methane volatile organic

compounds VOCs (NMVOCs) which are produced in the presence of nitrogen oxides ($NO_x = NO + NO_2$). These ozone precursors are emitted in large quantities due to human activities, such as traffic, fossil fuel combustion, industry, biomass burning, and non-human activities, such as lightning (Seinfeld and Pandis, 2006; Jacob, 2000).

30   The precursors can also interact with convective system, resulting in ozone production and transport at remote areas, many kilometers away from their source where it builds up (Sauvage et al., 2006). Tropospheric ozone has a lifetime of 22 ± 2 days (Stevenson et al., 2006). Through the production of hydroxyl and peroxy radicals (OH, RO_x), it influences the oxidizing power of the troposphere and affects the lifetime of other greenhouse gases such as methane CH_4 (Crutzen, 1974;

35   Shindell et al., 2009). In the lower troposphere ozone can be extremely harmful for human health as it can oxidize biological tissues and causes respiratory problems. Especially in smog events with abnormally high concentrations, it can be even deadly (WHO, 2006). On the other hand, ozone acts as a greenhouse gas in the upper troposphere, interacting with the up- and down-welling shortwave solar radiation and with the longwave terrestrial radiation (earthshine) (Stevenson et al., 2013). The

40   estimated radiative forcing (RF) due to tropospheric ozone is calculated to be 0.40 ± 0.20 Wm^{-2} (IPCC, 2013). Ozone is removed from the troposphere by several chemical reactions (3470 ± 520 $Tgyr^{-1}$) but it is also dry deposited (770 ± 180 $Tgyr^{-1}$) at the surface (IPCC, 2007). Nevertheless, the tropospheric ozone burden (300 ± 30 Tg (IPCC, 2007)) increases by 1-7% per decade in the tropics (Beig and Singh, 2007; Cooper et al., 2014) which makes the need to monitor it on a global scale

45   crucial.

Remote sensing from satellites has been proven to be very useful in providing consistent information of tropospheric ozone concentrations over large areas. Tropospheric ozone was first retrieved from space with the so-called residual method (Fishman et al., 1990). The stratospheric ozone column above 100 $mbar$ retrieved from the Stratospheric Aerosol and Gas Experiment II (SAGE II)

50   was subtracted from the total ozone column retrieved from the Total Ozone Mapping Spectrometer (TOMS) aboard the Nimbus 7 satellite. The following years several other methods have been developed, such as the cloud slicing (CS) technique (Ziemke et al., 2001). The later technique was first applied usng above cloud column ozone measurements from the Nimbus7 Total Ozone Mapping Spectrometer (TOMS) instrument in combination with Nimbus7 temperature-humidity and infrared

55   radiometer (THIR) cloud-top pressure data on TOMS. The CS takes advantage of the almost opaque property of water vapor clouds to ultraviolet wavelength radiation, in order to derive ozone column amounts in the upper troposphere. Later, the CS method was applied to ozone and cloud data from the Ozone Monitoring Instrument (OMI) (Ziemke et al., 2008) and from the Global Ozone Monitoring Experiment-2 (GOME-2) (Valks et al., 2014) to derive ozone mixing ratios inside Deep

60   Convective Clouds (DCC), and proved that very low ozone amounts exist inside these clouds over the Indian Ocean and the western Pacific Ocean. Kim et al. (2001) developed the Scan Angle Method (SAM) on TOMS data. The method was based on the physical differences in ozone column detec-

tion as a function of its scan-angle geometry. The difference in TOMS retrieval information between nadir and high viewing angles maximizes in the troposphere with a peak near an altitude of 5 km. This analysis suggests that the total ozone difference between two viewing angles contains information about tropospheric ozone. Another residual approach to retrieve tropospheric ozone has been applied to OMI total column ozone measurements in combination with Aura Microwave Limb Sounder (MLS) stratospheric column ozone measurements producing global maps of OMI/MLS tropospheric ozone (Ziemke et al., 2006). Tropospheric ozone data have been also produced with the Limb-Nadir-Matching (LNM) (Sierk et al., 2006; Ebojie et al., 2014) which benefits from the most important feature of SCIAMACHY, the possibility to observe the same atmospheric volume first in limb and then (after about 7 minutes) in nadir geometry. With the knowledge of the tropopause height, the tropospheric O_3 can be retrieved by subtracting the stratospheric (limb) from the total (nadir) O_3 columns. Equally important attempts to retrieve tropospheric ozone have been made using thermal infrared (TIR) emission instruments, such as the Infrared Atmospheric Sounding Interferometer (IASI) on MetOp-A (Keim et al., 2009; Boynard et al., 2009) or a combination of IR with ultraviolet (UV) measurements (Burrows et al., 2004; Cuesta et al., 1995).

The present study focuses on the Convective Cloud Differential (CCD) method which was first developed by Ziemke et al. (1998) and applied on TOMS (1979–2005) and OMI data (for 2004 and onwards) (Ziemke and Chandra, 2012). The same method was applied to GOME (Valks et al., 2003) and GOME-2 data (Valks et al., 2014). The technique uses above-cloud and clear-sky ozone column measurements to derive a monthly mean tropical tropospheric ozone column. The cloudy measurements above the Western Pacific and the Indian Ocean represent stratospheric ozone, which is assumed to be independent of longitude in the Tropics. Afterwards, the monthly mean Above Cloud Ozone Columns (ACCO) are subtracted from the cloud-free Total Ozone Columns (TOC), resulting in monthly averaged Tropical Tropospheric Columns of Ozone (TTCO). Here we present the application of our CCD algorithm (CCD_IUP) applied to the series of European satellite instruments GOME, SCIAMACHY, and GOME-2/MetopA spanning a time period of 16 years.

This manuscript is structured as follows. In section 2, we present the data that have been used in the CCD technique (total ozone, cloud fraction and cloud top height). In section 3, we describe the CCD technique and the modifications we made to the method applied in the past by Ziemke et al. (1998) and Valks et al. (2003, 2014). Section 4 presents the tropospheric ozone columns dataset (1996 to 2012) that has been created. First validation results from comparisons to ozonesondes and SCIAMACHY Limb Nadir Matching are presented and discussed in Section 4. Finally, section 5 provides a summary and conclusions.

2 The data

GOME (Burrows et al., 1999), SCIAMACHY (Bovensmann et al., 1999), and GOME-2 (Callies et al., 2000) are three European passive satellite instruments that have measured the back scattered and reflected electromagnetic radiation from the atmosphere in nadir viewing mode (Table 1). These
100   instruments have nearly identical spectral channels in the UV so that the same retrieval algorithm for total ozone and the derived tropospheric column ozone can be adopted without significant changes. While GOME and SCIAMACHY are already decommissioned, GOME-2 (METOP-A, launched in 2006) and GOME-2B (METOP-B, launched in 2012) still deliver data.

     The Weighting Function Differential Optical Absorption Spectroscopy (WFDOAS) is used to re-
105   trieve total ozone columns from nadir spectra in the UV window from 326 to 335 nm (Coldewey et al., 2005; Weber et al., 2004, 2013). The WFDOAS algorithm fits vertically integrated ozone weighting functions rather than ozone absorption cross-section to the sun-normalised radiances that enables a direct retrieval of vertical column amounts (Coldewey et al., 2005). The OCRA/ROCINN algorithms (Loyola et al., 2007) are used to derive cloud properties as cloud-top-height and cloud
110   fraction for GOME. This cloud information is used to correct the retrieved total ozone columns for not measurable ozone below clouds (Coldewey et al., 2005). These cloud properties are also used to infer the tropospheric ozone column (see below). A different cloud algorithm SACURA/OCRA (Kokhanovsky et al., 2005) is available for SCIAMACHY that retrieves cloud fraction (cf), cloud-top-height (cth), and other cloud parameters from the oxygen A-band (760 nm). In WFDOAS the
115   clouds are treated as Lambertian reflecting surfaces. The WFDOAS V2 has been also applied to GOME-2 spectral data (Weber et al., 2013) with the cloud properties being determined by the operational FRESCO+ algorithm (Wang et al., 2008). The agreement of WFDOAS total ozone for GOME and SCIAMACHY with ground data is within $\pm 1\%$ (Bracheret et al., 2005; Weber et al., 2004, 2013).

120   3 The CCD method

The Tropical Tropospheric Column of Ozone (TTCO) can be retrieved from satellite data with the Convective Clouds Differential (CCD) technique (Ziemke et al., 1998) using the total column of ozone and cloud information. The original technique, as applied to TOMS data, assumes that the ozone column above deep convective clouds (ACCO) simulates the stratospheric ozone in the same
125   latitude band and that this amount is invariant with latitude; which is approximately true in the tropics. However, a zonal variability on the order of ~ 5 DU (Fig. 2a) exists on monthly time scales in the tropical region. These differences may be influenced by episodic tropical waves (Kelvin waves, mixed Rossby-gravity waves, normal modes, and equatorial Rossby waves) in the stratosphere (Ziemke and Stanford, 1994). The CCD method is limited to the tropical belt.

130   For the calculation of the ACCO, all "cloudy " measurements are selected and monthly averaged in latitude bands of width 2.5° between -20° and 20° in the western Pacific and Indian Ocean (70°E-170°W). Fig. 1, illustrates the method and the considerations concerning the method that will be discussed later. This mean ACCO is then subtracted from the clear-sky (cf < 0.1) total ozone column (TCO) to derive the tropical tropospheric column of ozone (TTCO) in the same latitude band.

135   Several cloud fraction (cf) and cloud top heights (cth) thresholds where tested to define the "cloudy" measurements (see Fig. 2b). It was concluded that the ACCO does not change significantly when the cf is greater than 0.8 and cth greater than 7 km.

     The second basic assumption of the CCD method refers to the fact that the tropopause (∼18 km or ∼100 hPa) lies close to the top of the deep convective clouds (DCC). It is known that most DCC tops

140   only reach the bottom of the tropical tropopause layer or "tropical transition layer" (TTL) (Sherwood and Dessler, 2001; Gettelman and Forester, 2002; Fueglistaler et al., 2009), which is well below the thermal (cold point) tropopause (∼150 hPa). Only on rare occasions the DCCs overshoot the top of the TTL (Hong et al., 2007; Fueglistaler et al., 2009). These clouds are high, thick and bright with greatest occurrence rates over the ITCZ, the western Pacific, and the Indian Ocean (Sassen et

145   al., 2009; Hong et al., 2007). Fig. 3a shows the distribution of these clouds and their immigration following the ITCZ. In order to define the DCCs we used measurements with cloud fractions (cf) greater than 0.8 and cloud top heights (cth) greater than 9 km for SCIAMACHY and 7 km for GOME and GOME-2. Even with a higher cth threshold for SCIAMACHY, SCIAMACHY has the highest frequency of cloudy measurements among the three satellites (∼25%).

150   The original CCD method developed by Ziemke et al. (1998) assumed that UV nadir satellite measuring instruments measure ozone above the top of the DCC, something that is not completely true since UV radiation penetrates inside the cloud, resulting in an additional ozone absorption (Ziemke et al., 2008). Moreover, several cloud algorithms like FRESCO (Koelemeijer et al., 2001) and ROCINN (Loyola et al., 2007) assume that clouds behave as opaque Lambertian surfaces, resulting usually

155   in retrieving the effective (optical centroid) cloud top height (see Fig. 2 and 3) which lies below the physical cloud top height (Ziemke et al., 2008). SACURA cloud top height retrieval algorithm (Kokhanovsky et al., 2005) on the other hand takes into account radiative transfer inside, above and below the clouds (Lelli et al., 2014). Therefore, it provides more realistic cloud top heights. Fig. 3b shows that roughly ∼25% of cloud top heights in the western Pacific are higher than 9 km for

160   SACURA (SCIAMACHY) whereas for ROCINN (GOME-2), the same frequency is met for clouds only above 7 km. It is obvious that the different cloud algorithms calculate different cloud fractions and top heights and as a result yield different ACCO values. Therefore, a climatological correction term is applied to each individual measurement of ACCO in order to correct for different cloud top heights and adjust the ACCO to a fixed level of ∼ 200 hPa (12 km). This correction was also used

165   by Valks et al. (2014) although it is not documented in detail.

For the calculation of the vertical column (VC) which adjusts the ACCO values to the 200 hPa level, climatological ozone values from Fortuin and Kelder (1998) climatology where used. The Fortuin and Kelder (1998) climatology is reported in volume mixing ratios (vmr) for specific pressure levels. In order to convert the volume mixing ratios (ppm) to Dobson units (DU), the following
170 formula was used:

VC(i)=0.7889×0.5×[vmr(i)+vmr(i+1)]×[press(i)-press(i+1)]   (1)

Finally, the vertical ozone column of the nearest pressure level reported in climatology with each cloud top height (pressure) measurement was used for the adjustment of the ACCO.
 •If $ctp < 200$ hPa then $ACCO' = ACCO + VC$
175   •If $ctp > 200$ hPa then $ACCO' = ACCO - VC$
The ozone concentrations inside the high reflective clouds at the regions of the tropical eastern Indian Ocean and western Pacific are about 4–7 ppbv (corresponding to an ozone column of ~ 1 DU between the mean cloud top and the 200 hPa level). This is due to vertical convection of ozone poor oceanic air from the marine boundary layer into the upper troposphere so that the error from
180 ozone below the thermal tropopause is minimal if the retrieved ACCOs are taken from that region (Ziemke et al., 2008).

For this reason, for the cases where $ctp > 200$ hPa (for the reason discussed above, that ROCINN and FRESCO do not take into account the UV penetration inside the clouds), the value of 1 DU was subtracted from the climatological correction term in the case of GOME and GOME-2 ACCO. As
185 the geometrical top of the cloud is hundreds of meters higher than the one retrieved by FRESCO and ROCINN, the vertical ozone column correction between the cloud top height given from these algorithms and the 200 hPa is higher than it should.

Since the cloud algorithms differ between instruments and in order to have more than 50 cloudy ozone measurements per latitude band, the lower cloud top height limit classifying the DCCs is
190 different for each satellite instrument. For GOME and GOME-2 the minimum CTH is 7 km and for SCIAMACHY 9 km. All ACCO measurements which result in negative TTCOs or have a daily averaged standard deviation in a 2.5° lat by 5° lon bin of more than 10 DU or differ more than 4 DU with the neighbouring daily binned measurements are screened out. Finally, the monthly averaged ACCO per 2.5° latitude bands from the western Pacific region (70°E–170°W) is subtracted from
195 the monthly averaged total column (2.5° by 5° bins) of nearly cloud free areas (cf < 0.1), yielding the monthly tropical tropospheric column of ozone (TTCO). Fig. 4a shows the difference between the ACCO values before and after screening out the outliers. The differences are up to 10 DU for latitudes where less cloudy ozone measurements appear (in this case at Southern tropics, since the ITCZ moves to northern latitudes in summer, see Fig. 3a on the right for GOME-2). The ozone
200 column above than 200 hPa and three ozonesondes stations (Ascension, Kulala Lumpur and Hilo) is also presented in Fig. 4a. The ozonesonde burst altitude resides within the stratosphere, therefore the above 200 hPa ozone column form ozonesondes had to be indirectly calculated for these stations.

For this reason, the ozonesonde measurements from the surface up to 200 hPa were integrated and monthly averaged and then they where subtracted from the GOME-2 monthly averaged total ozone measurements, deriving the ozone column above 200 hPa. The agreement between the ozonesonde's ACCO and the corrected ACCO' is less than 2 DU. Finally, in the same figure the variation of the ACCO using 10 days and monthly averaging it is shown. In Fig. 4b is plotted the difference in ACCO between the western Pacific and the Atlantic basin. It is obvious that the ACCO values are overestimated over the Atlantic ocean (45°W–45°E) due to the existence of less high clouds and more polluted background from biomass burning that is up lifted to the UTLS (upper troposphere and lower stratosphere) region Sauvage et al. (2006); Avery et al. (2010).

4 Error analysis

This section summarizes the potential sources of uncertainty that contribute to the overall uncertainty in the retrieved tropical tropospheric ozone columns (TTCO). Table 2, 3 and 4 give an overview on all uncertainties that have been identified in TTCO retrieval for the year 2006, using SCIAMACHY ozone and cloud data. The propagation of these uncertainties to the TTCO is calculated as follows

$$X_{TTCO} = \sqrt{X_{TCO}^2 + X_{ACCO}^2} \tag{2}$$

as they are supposed to be uncorrelated and follow a Gaussian distribution. The assumption that the uncertainties are Gaussian distributed might lead to underestimation while the assumption that the errors are dependent and simply add up would significantly overestimate the actual uncertainty. The error in the total ozone column retrieval originates from the a-priori errors associated with the use of the ozone climatology and simplifying assumptions made in the derivation of effective parameters (Coldewey et al., 2005). Weber et al. (2004) showed that the monthly mean error in the total ozone column, $X_{TCO_{retrieval}}$ is about 1% ($\sim$2.6 DU). This error propagates in the total uncertainty. The monthly variability in the averaged total ozone column (1σ standard deviation of the mean), contributes randomly to the final total ozone column uncertainty. This parameter, σ_{TCO} is found to be $\sim$ 2 DU (0.8%) (see Table 2). The total uncertainty in the total ozone columns is therefore given by eq. 3 and is calculated to be less than 3.4 DU (1.3%, see Table 4).

$$X_{TCO} = \sqrt{X_{TCO_{retrieval}}^2 + \sigma_{TCO}^2} \tag{3}$$

However, the greatest uncertainty contribution in the tropospheric ozone column arises from the above cloud column calculation. The cloud knowledge is a parameter that introduces systematic errors in the ACCO retrieval. These uncertainties are inherent in every measurement and they affect the measurements selection criteria. In order to calculate the possible impact of cloud top height on the monthly mean ACCO, the ACCO values have been calculated using the marginal values of the known errors in cloud top height and cloud fraction detection. The deviation from the monthly mean ACCO using the reference values is then considered to be the parameter uncertainty for a given

parameter change (Rahpoe et al., 2013). The errors in the cloud top height estimation, X_{CTH} are about $\pm$ 500 m (Lelli L., 2013). Monthly ACCO values for cloud top heights greater than 8.5 km and 9.5 km were compared with the ACCO calculated for cloud tops greater than 9 km. Table 3

240 shows the uncertainty in ACCO due to cloud top height uncertainties. For the senario where cth $\geq$ 8.5 km, the uncertainty in ACCO is between $\sim$ 0.0 to 0.5 DU and for the scenario where the cth $\geq$ 9 km, the uncertainty in ACCO ranges between $\sim$ -0.8 to 0.7 DU. The error in cloud fraction, X_{CF} is $\pm$0.1 (Valks et al., 2011) which contributes to -0.4 to 0.8 DU in the ACCO uncertainty. The error in the ozone retrieval from WFDOAS, $X_{ACCO_{retrieval}}$ is also 1% and is added to the total uncertainty

245 of the ACCO. All these uncertainties are added up as shown follows.

$$X_{ACCO_{sys}} = \sqrt{X_{CTH}^2 + X_{CF}^2 + X_{ACCO_{retrieval}}^2} \qquad (4)$$

The hypothesis of the invariability of the ACCO through a latitude band introduces a random uncertainty ($X_{ACCO_{rand}}$) equal to the standard deviation (σ_{ACCO}) of each 2.5° lat gridbox in the reference region of the western Pacific (70°E-170°W). The uncertainty from the variability of the

250 ACCO within a latitude band has been calculated to be between 3–6 DU ($\sim$2%), whereas the systematic uncertainties are about 2.5 DU. The total ACCO uncertainty is calculated as follows

$$X_{ACCO} = \sqrt{X_{ACCO_{sys}}^2 + \sigma_{ACCO}^2} \qquad (5)$$

and ranges between 4–6.7 DU (1.8% – 2.8%) (see Table 4). Finally, the total tropospheric ozone (TTCO) uncertainty was calculated from eq. 2 and found to be between 5 to 7.4 DU (25 –36 %) as

255 summarized in Table 4.

5 Results

The CCD technique applied to GOME, SCIAMACHY and GOME-2 data provides consistent results with similar patterns and range of tropospheric ozone values (see Fig. 6a-c). All instruments exhibit the expected wave-one pattern of the tropical tropospheric ozone with high values over the South At-

260 lantic ($\sim$30-40 DU) and low values over the Indian and Pacific Oceans ($\sim$10-20 DU). This feature is persistent with a maximum in autumn (austral spring) which is a result of several reasons, such as the dynamical redistribution of ozone precursors from biomass burning from the African and South American continent to the mid-Atlantic. The main dynamical features in that region are the African Easterly Jet (AEJ) and the St-Helene high which leads to a redistribution of ozone from farther north

265 in Africa around Namibia (Diab et al., 2003). Whereas both the southwesterly Harmattan flow and the AEJ bring high ozone from the ground up to 600 hPa over the African continent, only the AEJ advection exports high ozone over the north Atlantic (Sauvage et al., 2006). Furthermore, upper tropospheric ozone production from lightning NO_x, sediments stronger over the southern tropical Atlantic as part of the Walker circulation and weaker over upwelling regions such as the tropical

270   Pacific (Martin et al., 2002). Tropospheric ozone over the tropical Pacific presents a persistent mini-
mum due to ozone loss reactions that are favoured by the specific conditions dominating there, such
as the high marine boundary layer air temperature and the low overhead ozone. These conditions
favor the strong advection from east to west by the Walker circulation. For this reason the tropo-
spheric air masses have been in a clean, warm and humid environment for a long time and loss of

275   odd oxygen, ozone and ozone precursors like $NO_x (= NO + NO_2, NO_x$ is lost by conversion into
HNO_3 followed by washout) proceeded longer than elsewhere in the tropics (Rex et al., 2014).

5.1   Validation with ozonesondes

The accuracy of the method was investigated by comparisons with collocated ozonesonde measure-
ments of tropospheric ozone columns ($\pm$ 5° in latitude and longitude). The data were taken from

280   the Southern Hemisphere ADditional OZonesondes (SHADOZ) network (Thompson et al., 2003).
The ozonesonde sites shown here (Fig. 7- 9), staring form North to South, are: (a) Hilo (19.4°N,
155.4°W), (b) Paramaribo (5.8°N, 55.2°W), (c) Kuala Lumpur (2.7°S, 101.7°E), (d) Nairobi (1.4°S,
36.8°E), (e) Natal (5.4°S, 35.4°W), (f) Java (7.6°S, 111°E), (g) Ascension (8°S, 14.4°W), (h) Samoa
(14.4°S, 170.6°W), and (i) Fiji (18.1°S, 178.4°E). We have selected the time-periods of 1996-2002

285   for GOME, 2003-2007 for SCIAMACHY and 2008-2012 for GOME-2 validation. For most stations,
the ozonesonde measurements start at 1998 and the launches vary from one to several per month (<
5). The ozone profiles were integrated until 200 hpa (bottom of the Tropical Transition Layer) and
the monthly mean and 1σ standard deviation calculated. No error bars are shown for stations with
only one launch per month. Ozonesondes provide measurements along the track of the sonde, which

290   could be transported several kilometers, whereas tropospheric ozone from CCD covers a larger area
(grid box of 2.5° by 5°).Tropospheric ozone can change from 30 to 70 ppbv within a convective cell
system (Avery et al., 2010). Considering these points and the fact that ozone sonde measurements
are rather sparse in time, the comparison of monthly averaged tropospheric ozone from CCD with
monthly averaged tropospheric ozone from ozonesondes has some limitations. Table 5 lists the time-

295   series mean GOME, SCIAMACHY, and GOME-2 TTCOs as well as tropospheric ozone columns
from ozonesondes at the statons mentioned above. Fig. 7 - 9 show the tropospheric ozone time-
series from the CCD method plotted with collocated ozonesondes measurements (until 200 hPa) for
the aforementioned stations. The comparison for all these ozonesonde stations, shows that the bias
is less than 5.2 DU, the mean biases range between 2 and 24%, the RMS between 4 and 10 DU,

300   and the correlation coefficient R ranges between 0.1 (Kuala Lumpur/GOME-2) and 0.8 (Ascension-
Natal/GOME-2). The average correlation coefficient for all sites and satellite instruments is about
0.6 (Fig. 10).

In more detail, Fig. 9a shows the comparison of tropospheric ozone column with ozonesondes in
Ascension island which is located in the South Atlantic. The correlation generally is weak, (with the

305   exception of GOME-2, where R=0.8) and the CCD method is found to consistently underestimate

the tropospheric ozone abundance at late summer/autumn months. The relative differences with ozonesondes are less than 14%. The mean tropospheric ozone values ($\sim$30 DU) are the highest among all the stations. The seasonal cycle is strong, with maximum in autumn (biomass burning season) and minimum in late Spring, when the ITCZ passes over the island and the wet season

310 begins. Similar seasonal cycle with slightly smaller mean values ($\sim$28 DU) can be seen in Natal (Fig. 8b), which is located 3400 km northwest of Ascension. The same seasonal discrepancy is also noticed here; however, the correlation coefficients are the greatest between all the stations, ranging from R=0.5 (GOME and SCIAMACHY) to R=0.8 (GOME-2), the bias is less than 2.9 DU (SCIAMACHY), and the relative difference is less than 11%. Paramaribo (Fig. 7b) is another station

315 in the Atlantic basin showing a distinct seasonal cycle (minimum at spring- maximum at autumn) but with even smaller mean tropospheric ozone values ($\sim$ 23 DU). The correlation with ozonesondes is moderate R= 0.5-0.6, the bias < 3 DU and the relative difference less than 12%.

On the other hand, Nairobi station (Fig. 8a) in Kenya, (central east Africa) shows even lower mean tropospheric ozone abundance ($\sim$25 DU) and very small seasonal variations. The reduced seasonal

320 cycle can be explained by the location of Nairobi being away from the southwest continental outflow due to the Harmattan winds. The correlation with ozonesondes in Nairobi is weak for all instruments (R < 0.3) but the biases (< 1 DU for GOME and SCIAMACHY and < 3.4 DU for GOME-2) the RMS ($\sim$5 DU) and the relative differences (< 13%) are satisfactory low.

The CCD results for the Indian ocean stations such as Kuala Lumpur and Java (Fig. 7c and 8c),

325 show very low mean tropospheric ozone values ($\sim$19 DU). The ozone abundance gets even lower (< 10 DU) in summer months (particularly in the case of SCIAMACHY and GOME retrievals) when the monsoon season is active and the ITCZ moves northwards. The South East Trade winds of the Southern Hemisphere crossing the equator are deflected eastwards in the Northern Hemisphere due to the Coriolis effect, yielding into the C-shape monsoon winds blowing from the South-West

330 direction in the lower troposphere (Loschnigg and Webster, 2000; Yonemura et al., 2002). As a result, clean ozone air reaches the Indonesian-Malaysian Peninsula. The opposite circulation takes place in winter, where the gradient is turning from South to North bringing polluted continental air to both sites. The correlation with the Indian ocean stations is weak (R < 0.5) since tropospheric ozone is low, the seasonal cycle weak or even non existent. The bias is less than 7 DU. Enhanced

335 ozone levels at Java station (Watukosek) can be seen in the midwinter months of 1997, 2002, 2004, 2006 and 2009 (October-January) due to El Niño conditions (Ziemke et al., 2010). El Niño is linked to changes in the convection pattern (less clouds over Indonesian region) and increase of biomass burning (Valks et al., 2014).

Correlation for the Pacific Ocean sites Fiji and Hilo (Fig. 9C and 7a) is moderate (R $\sim$0.5) with

340 biases less than 2.4 DU in most cases. The RMS is excessively large (>8.6 DU) and the tropospheric ozone values are among the greatest ($\sim$29 DU) in Hilo which is located in the northern hemisphere, where stratospheric intrusions via tropopause foldings are more possible than at other stations. Tro-

pospheric ozone values at Fiji are maximum at summer and minimum at winter opposite to Hilo. After 2006 there are larger gaps in the Fiji ozonesonde data record. The movement of the ITCZ

345 causes less cloudy measurements to appear at summer months in Fiji and winter months in Hilo since both stations are located near the southern and northern boundary of the tropical region. As a result the ACCO measurements are considered to be statistically doubtful and no TTCO is retrieved for that cases. Fig. 9b presents the tropospheric ozone at Samoa island which ranges around 21 DU with slightly higher values in autumn. The comparison of CCD and ozonesondes at Samoa shows

350 that CCD mainly overestimates the retrieved tropospheric ozone. The bias (< 5.2 DU) is small, whereas the relative differences (14-24%) and RMS (< 7 DU) are large, and the correlation is weak (R < 0.4).

5.2 Comparison with Limb/Nadir Matching tropospheric ozone columns

Tropospheric ozone columns from Limb/Nadir Matching (LNM) observations of SCIAMACHY

355 instrument are available (Ebojie et al., 2014). The monthly mean tropospheric ozone columns have in general errors of less than 6 DU, whereas the comparison with collocated and integrated ozonesonde profiles up to the tropopause, shows agreement within $2 - 5$ DU (Ebojie et al., 2014). In order to make the comparison with Tropospheric ozone columns from CCD method with LNM more realistic, 10% of the LNM ozone columns have been subtracted to account for the ozone between 200 hPa

360 (assuming a constand volumn mixing ratio) and the tropopause that is missing in CCD but contained in LNM TCO. Here, we present the comparison between CCD, LNM and collocated ozonesonde profiles (until 200 hPa) for six sites ((a) Paramaribo (5.8°N, 55.2°W), (b) Kuala Lumpur (2.7°S, 101.7°E), (c) Nairobi (1.4°S, 36.8°E), (d) Natal (5.4°S, 35.4°W), (e) Samoa (14.4°S, 170.6°W), and (f) Ascension (8°S, 14.4°W)) between January 2004 and December 2011 (Fig. 11). It is apparent

365 that the LNM tropospheric ozone columns appear somewhat noisier, exhibiting some anticorrelated peaks with respect to ozonesondes (e.g. Kuala Lumpur, Paramaribo, Samoa). On the other hand, the seasonality and the range of ozone values is well followed at stations with a distinct seasonal cycle (Natal, Ascension). Both CCD and LNM tropospheric ozone columns exhibit weak to low correlation (R<0.5) and differences of less than 10% with the exception of Nairobi where relative

370 difference is 22% (see Table 6). CCD generally agrees better with ozonesondes (0.3 < R < 0.7) with the exception of Nairobi and Samoa. Finally, there is no correlation between the three datasets at Kuala Lumpur.

6 Conclusions

Monthly averaged tropospheric ozone columns have been calculated on a 2.5° latitude by 5° longi-

375 tude grid between 20°S – 20°N using the CCD method from 1996 – 2012 for GOME/ERS-2, SCIA-MACHY/ENVISAT and GOME-2/MetopA data. The method indicates that the retrieved ACCO

provides a reasonable approximation of the stratospheric ozone columns despite the assumptions
and corrections done in the ACCO calculation, although there are limitations due to cases of lim-
ited cloudy data in some latitude bands as a result of the ITCZ seasonal migration. The comparison
380 with nine SHADOZ ozonesonde sites shows moderate agreement with a mean correlation coeffi-
cient of R=0.6 for all instruments. The biases are generally less than 5 DU, RMS are less than 10
DU and relative differences do not exceed 24% (within the uncertainty range). Further optimization
of the WFDOAS data (use of SACURA/OCRA algorithm for cloud properties for all satellite data)
and extension to GOME-2/MetopB is planned in order to improve the consistency between satel-
385 lite datasets for long-term trend and variability studies. The comparison with limb-nadir-matching
observations from SCIAMACHY show good agreement, however the monthly mean differences to
SHADOZ ozonesondes show somewhat larger variability in the LNM data than CCD data.

In summary, this unique 17 year tropical tropospheric ozone dataset provides valuable information
about the tropospheric ozone distribution. These long-term tropospheric ozone timeseries can be
390 used in climate models and tropospheric ozone trend studies.

Acknowledgements. This work was supported in parts by the DLR S5P project (50EE1247) and the federal
state of Bremen.

References

Avery, M., Twohy, C., McCabe, D., Joiner, J., Severance, K., Atlas, E., Blake, D., Bui, T. P., Crounse, J.,
Dibb, J., Diskin, G., Lawson, P., McGill, M., Rogers, D., Sachse, G., Scheuer, E., Thompson, A. M., Trepte,
C., Wennberg, P. and Ziemke, J.: Convective distribution of tropospheric ozone and tracers in the Cen-
tral American ITCZ region: Evidence from observations during TC4, J. Geophys. Res. Atmos., 115(19),
doi:10.1029/2009JD013450, 2010.

Beig, G. and Singh, V.: Trends in tropical tropospheric column ozone from satellite data and MOZART model,
Geophys. Res. Lett., 34(17), L17801, doi:10.1029/2007GL030460, 2007.

Bovensmann, H., Burrows, J. P., Buchwitz, M., Frerick, J., Noël, S., Rozanov, V. V., Chance, K. V. and Goede,
A. P. H.: SCIAMACHY: Mission Objectives and Measurement Modes, J. Atmos. Sci., 56(2), 127-150,
doi:10.1175/1520-0469(1999)056<0127:SMOAMM>2.0.CO;2, 1999.

Boynard, A., Clerbaux, C., Coheur, P.-F., Hurtmans, D., Turquety, S., George, M., Hadji-Lazaro, J., Keim, C.,
and Meyer-Arnek, J.: Measurements of total and tropospheric ozone from IASI: comparison with correlative
satellite, ground-based and ozonesonde observations, Atmos. Chem. Phys., 9, 6255-6271, doi:10.5194/acp-
9-6255-2009, 2009

Bracher, a., Weber, M., Bramstedt, K., Coldewey-Egbers, M., Lamsal, L. N. and Burrows, J. P.: Global satellite
validation of SCIAMACHY O3 columns with GOME WFDOAS, Atmos. Chem. Phys. Discuss., 5(1), 795-
813, doi:10.5194/acpd-5-795-2005, 2005.

Burrows, J. P., Weber, M., Buchwitz, M., Rozanov, V., Ladstätter-Weißenmayer, A., Richter, A., DeBeek, R.,
Hoogen, R., Bramstedt, K., Eichmann, K.-U., Eisinger, M. and Perner, D.: The Global Ozone Monitor-
ing Experiment (GOME): Mission Concept and First Scientific Results, J. Atmos. Sci., 56(2), 151-175,
doi:10.1175/1520-0469(1999)056<0151:TGOMEG>2.0.CO;2, 1999.

Burrows, J. P., Bovensmann, H., Bergametti, G., Flaud, J. ., Orphal, J., Noël, S., Monks, P. ., Corlett, G. ., Goede,
A. ., von Clarmann, T., Steck, T., Fischer, H. and Friedl-Vallon, F.: The geostationary tropospheric pollution
explorer (GeoTROPE) mission: objectives, requirements and mission concept, Adv. Sp. Res., 34(4), 682-687,
doi:10.1016/j.asr.2003.08.067, 2004.

Callies, J., Corpaccioli, E. and Eisinger, M., Hahne, A. and Lefebvre, A.: GOME-2 - Metop-s second-generation
sensor for operational ozone monitoring, ESA Bull. Sp. Agency, 102, 28-36, 2000.

Coldewey-Egbers, M., Weber, M., Lamsal, L. N., de Beek, R., Buchwitz, M. and Burrows, J. P.: Total ozone
retrieval from GOME UV spectral data using the weighting function DOAS approach, Atmos. Chem. Phys.,
5(4), 1015-1025, doi:10.5194/acp-5-1015-2005, 2005.

Cooper, O. R., Parrish, D. D., Ziemke, J., Balashov, N. V., Cupeiro, M., Galbally, I. E., Gilge, S., Horowitz,
L., Jensen, N. R., Lamarque, J.-F., Naik, V., Oltmans, S. J., Schwab, J., Shindell, D. T., Thompson, A.
M., Thouret, V., Wang, Y. and Zbinden, R. M.: Global distribution and trends of tropospheric ozone: An
observation-based review, Elem. Sci. Anthr., 2, 000029, doi:10.12952/journal.elementa.000029, 2014.

Crutzen, P. J.: Photochemical reactions initiated by and influencing ozone in unpolluted tropospheric air, Tellus
A, 26(1-2), doi:10.3402/tellusa.v26i1-2.9736, 1974.

Crutzen, P. J.: Ozone in the troposphere, in Composition, Chemistry, and Climate of the Atmosphere, pp. 349-
393, Reinhold N., New York., 1995.

Cuesta, J., Eremenko, M., Liu, X., Dufour, G., Hoepfner, M., Cai, Z., von Clarmann, T., Orphal, J., Chance, K., Spurr, R., Flaud, J. M. and Giesen, N.: Multi-spectral retrieval of lowermost tropospheric ozone combining IASI and GOME-2 satellite observations, EGU Gen. Assem. Conf. Abstr., 14, 10849 [online] Available from: http://adsabs.harvard.edu/abs/2012EGUGA..1410849C, 2012.

Diab, R. D., Raghunandan, A., Thompson, A. M. and Thouret, V.: Classification of tropospheric ozone profiles over Johannesburg based on MOZAIC aircraft data, Atmos. Chem. Phys. Discuss., 3(1), 705-732, doi:10.5194/acpd-3-705-2003, 2003.

Ebojie, F., von Savigny, C., Ladstätter - Weißenmayer, a., Rozanov, a., Weber, M., Eichmann, K., Bötel, S., Rahpoe, N., Bovensmann, H., and Burrows, J. P.: Tropospheric column amount of ozone retrieved from SCIAMACHY limb–nadir-matching observations, Atmos. Meas. Tech., 7, 2073-2096, doi:10.5194/amt-7-2073-2014, 2014.

Fishman, J., Watson, C. E., Larsen, J. C. and Logan, J. A.: Distribution of tropospheric ozone determined from satellite data, J. Geophys. Res., 95(D4), 3599, doi:10.1029/JD095iD04p03599, 1990.

Fortuin, P.J.F. and Kelder, H.: An ozone climatology based on ozonesonde and satellite measurements, J. Geophys. Res., 103(D24), 31709–31734, doi:10.1029/1998JD200008, 1998.

Fueglistaler, S., Dessler, A. E., Dunkerton, T. J., Folkins, I., Fu, Q. and Mote, P. W.: Tropical tropopause layer, Rev. Geophys., 47(1), RG1004, doi:10.1029/2008RG000267, 2009.

Jacob, D. J.: Introduction to Atmospheric Chemistry, Princeton University Press., 2000.

Jia, J., Rozanov, A., Ladstätter - Weißenmayer, A., and P. Burrows, J.: Global validation of improved SCIA-MACHY scientific ozone limb data using ozonesonde measurements, Atmos. Meas. Tech. Discuss., 8, 4817-4858, doi:10.5194/amtd-8-4817-2015, 2015.

Gettelman, A. and Forester, P. M. de F.: A Climatology of the Tropical Tropopause Layer., J. Meteorol. Soc. Japan, 80(4B), 911-924, doi:10.2151/jmsj.80.911, 2002.

Hong, G., Yang, P., Gao, B.-C., Baum, B. A., Hu, Y. X., King, M. D. and Platnick, S.: High Cloud Properties from Three Years of MODIS Terra and Aqua Collection-4 Data over the Tropics, J. Appl. Meteorol. Climatol., 46(11), 1840-1856, doi:10.1175/2007JAMC1583.1, 2007.

IPCC: Climate Change 2007 - The Physical Science Basis: Working Group I Contribution to the Fourth Assessment Report of the IPCC (Climate Change 2007). [online] Available from: http://www.amazon.ca/exec/obidos/redirect-tag=citeulike09-20&, 2007.

IPCC Working Group 1, I., Stocker, T. F., Qin, D., Plattner, G.-K., Tignor, M., Allen, S. K., Boschung, J., Nauels, A., Xia, Y., Bex, V. and Midgley, P. M.: IPCC, 2013: Climate Change 2013: The Physical Science Basis. Contribution of Working Group I to the Fifth Assessment Report of the Intergovernmental Panel on Climate Change, IPCC, AR5, 1535, 2013.

Keim, C., Eremenko, M., Orphal, J., Dufour, G., Flaud, J.-M., Höpfner, M., Boynard, A., Clerbaux, C., Payan, S., Coheur, P.-F., Hurtmans, D., Claude, H., Dier, H., Johnson, B., Kelder, H., Kivi, R., Koide, T., López Bartolomé, M., Lambkin, K., Moore, D., Schmidlin, F. J., and Stübi, R.: Tropospheric ozone from IASI: comparison of different inversion algorithms and validation with ozone sondes in the northern middle latitudes, Atmos. Chem. Phys., 9, 9329-9347, doi:10.5194/acp-9-9329-2009, 2009.

470   Kim, J. H., Newchurch, M. J. and Han, K.: Distribution of Tropical Tropospheric Ozone Determined by the
            Scan-Angle Method Applied to TOMS Measurements, J. Atmos. Sci., 58(18), 2699-2708, doi:10.1175/1520-
            0469(2001)058<2699:DOTTOD>2.0.CO;2, 2001.

        Koelemeijer, R. B. A., Stammes, P., Hovenier, J. W. and de Haan, J. F.: A fast method for retrieval of cloud
            parameters using oxygen A band measurements from the Global Ozone Monitoring Experiment, J. Geophys.
475   Res., 106(D4), 3475, doi:10.1029/2000JD900657, 2001.

        Kokhanovsky, A. A., Rozanov, V. V., Burrows, J. P., Eichmann, K.-U., Lotz, W. and Vountas, M.: The
            SCIAMACHY cloud products: Algorithms and examples from ENVISAT, Adv. Sp. Res., 36(5), 789-799,
            doi:10.1016/j.asr.2005.03.026, 2005.

        Studies of global cloud field using measurements of GOME, SCIAMACHY and GOME-2, PhD Thesis, Institute
480   of Environmental Physics, University of Bremen, Otto-Hahn-Allee 1, 28334, Bremen, Germany, 2013.

        Lelli, L., Kokhanovsky, A. A., Rozanov, V. V., Vountas, M., and Burrows, J. P.: Linear trends in cloud top height
            from passive observations in the oxygen A-band, Atmos. Chem. Phys., 14, 5679-5692, doi:10.5194/acp-14-
            5679-2014, 2014.

        Loschnigg, J. and Webster, P. J.: A Coupled Ocean-Atmosphere System of SST Modulation for the Indian
485   Ocean*, J. Clim., 13(19), 3342-3360, doi:10.1175/1520-0442(2000)013<3342:ACOASO>2.0.CO;2, 2000.

        Loyola, D. G., Thomas, W., Livschitz, Y., Ruppert, T., Albert, P. and Hollmann, R.: Cloud Properties Derived
            From GOME/ERS-2 Backscatter Data for Trace Gas Retrieval, IEEE Trans. Geosci. Remote Sens., 45(9),
            2747-2758, doi:10.1109/TGRS.2007.901043, 2007.

        Martin, R. V.: Interpretation of TOMS observations of tropical tropospheric ozone with a global model and in
490   situ observations, J. Geophys. Res., 107(D18), 4351, doi:10.1029/2001JD001480, 2002.

        Rahpoe, N., von Savigny, C., Weber, M., Rozanov, A.V., Bovensmann, H., and Burrows, J. P.: Error budget
            analysis of SCIAMACHY limb ozone profile retrievals using the SCIATRAN model, Atmos. Meas. Tech.,
            6, 2825-2837, doi:10.5194/amt-6-2825-2013, 2013.

        Rex, M. , Wohltmann, I. , Ridder, T. , Lehmann, R. , Rosenlof, K. , Wennberg, P. , Weisenstein, D. K. , Notholt,
495   J. , Krüger, K. , Mohr, V. and Tegtmeier, S.: A Tropical West Pacific OH Minimum and Implications for
            Stratospheric Composition , Atmospheric Chemistry and Physics, 14 (9), pp. 4827-4841 . doi: 10.5194/acp-
            14-4827-2014, 2014.

        Sassen, K., Wang, Z. and Liu, D.: Cirrus clouds and deep convection in the tropics: Insights from CALIPSO
            and CloudSat, J. Geophys. Res., 114(21), D00H06, doi:10.1029/2009JD011916, 2009.

500   Sauvage, B., V. Thouret, A. M. Thompson, J. C. Witte, J.-P. Cammas, P. Nédélec, and G. Athier:, Enhanced
            view of the "tropical Atlantic ozone paradox" and "zonal wave one" from the in situ MOZAIC and SHADOZ
            data, J. Geophys. Res., 111, D01301, doi:10.1029/2005JD006241, 2006.

        Seinfeld, J. H. and Pandis, S. N.: Atmospheric Chemistry and Physics: From Air Pollution to Climate Change.
            [online] Available from: http://www.amazon.com/dp/0471178160, 2006.

505   Shindell, D. T., Faluvegi, G., Koch, D. M., Schmidt, G. a, Unger, N. and Bauer, S. E.: Improved attribution of
            climate forcing to emissions., Science, 326(5953), 716-8, doi:10.1126/science.1174760, 2009.

        Sierk, B., Richter, A., Rozanov, A., Savigny, C. Von, Schmoltner, A. M., Buchwitz, M., Bovensmann, H.
            and Burrows, J. P.: Retrieval And Monitoring of Atmospheric Trace Gas Concentrations in Nadir and

Limb Geometry Using the Space-Borne Sciamachy Instrument, Environ. Monit. Assess., 120(1-3), 65-77,
510 doi:10.1007/s10661-005-9049-9, 2006.

Sherwood, S. C. and Dessler, A. E.: A model for transport across the tropical tropopause, J. Atmos. Sci., 58(7),
 765-779 [online] Available from: <Go to ISI>://000167550300006, 2001.

Stevenson, D.S., F.J. Dentener, M.G. Schultz, K. Ellingsen, T.P.C. van Noije, O. Wild, G. Zeng, M. Amann, C.S.
 Atherton, N. Bell, D.J. Bergmann, I. Bey, T. Butler, J. Cofala, W.J. Collins, R.G. Derwent, R.M. Doherty,
515 J. Drevet, H.J. Eskes, A.M. Fiore, M. Gauss, D.A. Hauglustaine, L.W. Horowitz, I.S.A. Isaksen, M.C. Krol,
 J.F. Lamarque, M.G. Lawrence, V. Montanaro, J.F. Müller, G. Pitari, M.J. Prather, J.A. Pyle, S. Rast, J.M.
 Rodriguez, M.G. Sanderson, N.H. Savage, D.T. Shindell, S.E. Strahan, K. Sudo, and S. Szopa: Multimodel
 ensemble simulations of present-day and near-future tropospheric ozone. J. Geophys. Res., 111, D08301,
 doi:10.1029/2005JD006338, 2006.

520 Stevenson, D. S., Young, P. J., Naik, V., Lamarque, J.-F., Shindell, D. T., Voulgarakis, a., Skeie, R. B., Dalsoren,
 S. B., Myhre, G., Berntsen, T. K., Folberth, G. a., Rumbold, S. T., Collins, W. J., MacKenzie, I. a., Doherty,
 R. M., Zeng, G., van Noije, T. P. C., Strunk, a., Bergmann, D., Cameron-Smith, P., Plummer, D. a., Strode,
 S. a., Horowitz, L., Lee, Y. H., Szopa, S., Sudo, K., Nagashima, T., Josse, B., Cionni, I., Righi, M., Eyring,
 V., Conley, a., Bowman, K. W., Wild, O. and Archibald, a.: Tropospheric ozone changes, radiative forc-
525 ing and attribution to emissions in the Atmospheric Chemistry and Climate Model Intercomparison Project
 (ACCMIP), Atmos. Chem. Phys., 13(6), 3063-3085, doi:10.5194/acp-13-3063-2013, 2013.

Thompson, A.M., et al.: Southern Hemisphere Additional Ozonesondes (SHADOZ) 1998-2000 tropical ozone
 climatology 1. Comparison with Total Ozone Mapping Spectrometer (TOMS) and ground-based measure-
 ments, J. Geophys. Res., 108, 8238, doi:10.1029/2001JD000967, 2003.

530 Valks, P. J. M.: Variability in tropical tropospheric ozone: Analysis with Global Ozone Monitoring Experiment
 observations and a global model, J. Geophys. Res., 108(D11), 4328, doi:10.1029/2002JD002894, 2003.

Valks, P., Loyola, D., Hao, N., Rix, M., and Slijkhuis, S.: Algorithm Theoretical Basis Document for GOME-2
 Total Column Products of Ozone, Minor Trace Gases and Cloud Properties(GDP 4.5 for O3M-SAF OTO
 and NTO), DLR/GOME-2/ATBD/01, Iss./Rev.: 2/E, available at: http://atmos.eoc.dlr.de/gome2/docs/DLR_
535 GOME-2_ATBD.pdf, 2011.

Valks, P., Hao, N., Gimeno Garcia, S., Loyola, D., Dameris, M., Jöckel, P. and Delcloo, A.: Tropical tropospheric
 ozone column retrieval for GOME-2, Atmos. Meas. Tech. Discuss., 7(1), 727-768, doi:10.5194/amtd-7-727-
 2014, 2014.

Wang, P., Stammes, P., van der A, R., Pinardi, G., and van Roozendael, M.: FRESCO+: an improved O2
540 A-band cloud retrieval algorithm for tropospheric trace gas retrievals, Atmos. Chem.Phys., 8, 6565-6576,
 doi:10.5194/acp-8-6565-2008, 2008.

Weber, M., Lamsal, L. N., Coldewey-Egbers, M., Bramstedt, K. and Burrows, J. P.: Pole-to-pole validation
 of GOME WFDOAS total ozone with groundbased data, Atmos. Chem. Phys. Discuss., 4(5), 6909-6941,
 doi:10.5194/acpd-4-6909-2004, 2004.

545 Weber, M., W. Chehade, V. E. Fioletov, S. M. Frith, C. S. Long, W. Steinbrecht, J. D. Wild, [Global Climate]
 Stratospheric ozone [in "State of the Climate in 2012"], Bull. Amer. Meteor. Soc., 94, S36-S37, 2013

W. H. O.: Health risks of particulate matter from long-range transboundary air pollution. [online] Available
 from:http://www.euro.who.int/data/assets/pdf_file/0006/78657/E88189.pdf, 2006.

Yonemura, S., H. Tsuruta, S. Kawashima, S. Sudo, L. C. Peng, L. S. Fook, Z. Johar, and M. Hayashi, Tropospheric ozone climatology over Peninsular Malaysia from 1992 to 1999, J. Geophys. Res., 107(D15), doi:10.1029/2001JD000993, 2002.

Ziemke, J. R. and Stanford, J. L.: Kelvin waves in total column ozone, Geophys. Res. Lett., 21(2), 105-108, doi:10.1029/93GL03287, 1994.

Ziemke, J. R., Chandra, S. and Bhartia, P. K.: Two new methods for deriving tropospheric column ozone from TOMS measurements: Assimilated UARS MLS/HALOE and convective-cloud differential techniques, J. Geophys. Res., 103(D17), 22115, doi:10.1029/98JD01567, 1998.

Ziemke, J. R., S. Chandra, and P. K. Bhartia: "Cloud slicing": A new technique to derive upper tropospheric ozone from satellite measurements, J. Geophys. Res., 106(D9), 9853-9867, doi:10.1029/2000JD900768, 2001.

Ziemke, J. R., S. Chandra, B. N. Duncan, L. Froidevaux, P. K. Bhartia, P. F. Levelt, and J. W. Waters: Tropospheric ozone determined from Aura OMI and MLS: Evaluation of measurements and comparison with the Global Modeling Initiative's Chemical Transport Model, J. Geophys. Res., 111, D19303, doi:10.1029/2006JD007089, 2006.

Ziemke, J. R., Joiner, J., Chandra, S., Bhartia, P. K., Vasilkov, A., Haffner, D. P., Yang, K., Schoeberl, M. R., Froidevaux, L. and Levelt, P. F.: Ozone mixing ratios inside tropical deep convective clouds from OMI satellite measurements, Atmos. Chem. Phys. Discuss., 8(4), 16381-16407, doi:10.5194/acpd-8-16381-2008, 2008.

Ziemke, J. R., Chandra S., Oman L. D., and Bhartia P. K.: A new ENSO index derived from satellite measurements of column ozone, Atmos. Chem. Phys., 10, 3711-3721, doi:10.5194/acp-10-3711-2010, 2010.

Ziemke, J. R. and Chandra, S.: Development of a climate record of tropospheric and stratospheric column ozone from satellite remote sensing: evidence of an early recovery of global stratospheric ozone, Atmos. Chem. Phys., 12, 5737-5753, doi:10.5194/acp-12-5737-2012, 2012.

List of Tables

List of Figures

Table 1. Characteristics of the satellite instruments used

Instruments	GOME/ERS-2	SCIAMACHY/ENVISAT	GOME-2/METOP-A
Data period	06/1995-07/2011*	08/2002-04/2012	01/2007-present
Spectral Coverage	240 - 790 nm	240 - 2380 nm	240 - 790 nm
Ground pixel size	320 x 40 km^2	60 x 30 km^2	40 x 80 km^2
Equator crossing time	10:30 a.m.	10:00 a.m.	9:30 a.m.
Global coverage	3 days	6 days	almost daily

(∗) GOME global coverage lost in June 2003

Table 2. Monthly average of Total ozone column parameter uncertainties in 2006. Denoted with σ is the assumed parameter uncertainty

Month	Uncertainty in TCO due to monthly variability (σ_{TCO})		Error in ozone retrieval $(X_{TCO_{retrieval}})$	
	(DU)	%	(DU)	%
January	2.0	0.8	2.5	1
February	2.0	0.8	2.5	1
March	2.1	0.8	2.5	1
April	2.0	0.8	2.6	1
May	2.1	0.8	2.6	1
June	2.1	0.8	2.6	1
July	2.1	0.8	2.7	1
August	2.1	0.8	2.7	1
September	2.1	0.8	2.7	1
October	2.1	0.8	2.7	1
November	2.0	0.8	2.6	1
December	2.0	0.8	2.5	1

Table 3. Monthly average of above cloud column ozone (ACCO) uncertainties per 2.5° lat bins in 2006.

Month	Uncertainty in cloud top height $(X_{CTH}=$ +500m)		Uncertainty in cloud top height $(X_{CTH}=$ -500m)		Uncertainty in cloud fraction $(X_{CF}=$ +0.1)		Error in cloud fraction $(X_{CF}=$ -0.1)		Uncertainty in ACCO due to latitudinal deviation (σ_{ACCO})		Error in ozone retrieval $(X_{ACCO_{retrieval}})$	
	(DU)	%	(DU)	%	(DU)	%	(DU)	%	(DU)	%	(DU)	%
January	0.2	0.1	-0.2	-0.1	-0.3	-0.1	0.1	0.0	6.2	2.6	2.4	1
February	0.2	0.1	-0.1	0.0	0.7	0.3	0.4	0.2	4.8	2.0	2.4	1
March	0.1	0.0	-0.1	0.0	0.0	0.0	-0.3	-0.1	4.1	1.8	2.3	1
April	0.2	0.1	-0.1	0.0	0.1	0.0	0.1	0.0	4.0	1.7	2.3	1
May	0.2	0.1	-0.2	-0.1	-0.2	-0.1	0.5	0.2	4.1	1.8	2.3	1
June	0.1	0.0	-0.2	-0.1	-0.3	-0.1	0.4	0.2	3.7	1.6	2.3	1
July	0.1	0.0	-0.3	-0.1	-0.1	0.0	0.2	0.1	3.4	1.5	2.3	1
August	0.1	0.0	-0.4	-0.2	0.1	0.0	0.6	0.3	4.0	1.8	2.3	1
September	0.3	0.1	-0.1	0.0	0.0	0.0	0.6	0.3	3.8	1.7	2.3	1
October	0.5	0.2	-0.2	-0.1	-0.3	-0.1	0.8	0.4	5.3	2.4	2.2	1
November	0.2	0.1	-0.3	-0.1	-0.4	-0.2	0.6	0.3	4.5	2.0	2.2	1
December	0.0	0.0	-0.2	-0.1	-0.8	-0.4	0.2	0.1	3.2	1.5	2.2	1

Table 4. Monthly average and uncertainties in tropospheric ozone column (TTCO) due to the uncertainties in total ozone column (TCO) and the above cloud column ozone (ACCO).

Month	Mean Tropical Tropospheric Column of Ozone (TTCO)	Uncertainty in TTCO (X_{TTCO})		Mean Above Cloud Column of Ozone (ACCO)	Uncertainty in ACCO (X_{ACCO})		Mean Total Column of Ozone (TCO)	Uncertainty in TCO (X_{TCO})	
	(DU)	(DU)	%	(DU)	(DU)	%	(DU)	(DU)	%
January	20.6	7.4	35.8	237.6	6.7	2.8	246.2	3.2	1.3
February	19.5	6.3	32.2	236.5	5.4	2.3	246.2	3.2	1.3
March	19.2	5.7	29.8	233.5	4.7	2.0	253.6	3.3	1.3
April	18.7	5.7	30.5	232.5	4.6	2.0	258.4	3.3	1.3
May	16.8	5.8	34.5	230.7	4.7	2.1	260.9	3.3	1.3
June	21.0	5.5	26.4	229.4	4.4	1.8	263.8	3.4	1.3
July	20.3	5.3	26.3	228.4	4.1	2.5	266.5	3.4	1.3
August	21.7	5.8	26.5	228.1	4.7	2.0	268.0	3.4	1.3
September	21.1	5.6	26.5	226.7	4.5	2.0	269.1	3.4	1.3
October	21.0	6.7	32.1	224.8	5.8	2.6	261.8	3.3	1.3
November	19.4	6.0	31.2	221.0	5.1	2.3	256.7	3.3	1.3
December	20.6	5.1	24.8	216.2	4.0	1.8	247.6	3.2	1.3

Table 5. Statistical comparison between a) GOME, SCIAMACHY, and GOME-2 TTCOs with ozoneson-des for nine SHADOZ sites. Information presented here: the ozonesonde site, the mean TTCO for GOME/SCIAMACHY and for ozonesondes, the relative difference, the bias and the RMS difference between CCD TTCO and sondes and finally the correlation coefficient. The values are in DU.

Site (1996-2002)	GOME TTCO (DU)	SONDES TTCO (DU)	Relative difference	BIAS (DU)	RMS (DU)	R
Hilo (19.4N,155.4W)	28.4	26.4	0.07	2.0	9.2	0.5
Paramaribo (5.8N,55.2W)	22.4	24.1	0.07	-1.7	3.9	0.6
Kuala Lumpur (2.7N,101.7E)	16.7	19.1	0.14	-2.5	5.4	0.4
Nairobi (1.3S,36.8E)	22.8	23.6	0.04	-0.8	5.2	0.3
Natal (5.4S,35.4W)	27.1	28.0	0.03	-0.9	6.9	0.5
Java (7.6S,111E)	18.8	19.6	0.04	-0.7	4.8	0.4
Ascension (8S,14.4W)	30.5	32.9	0.07	-2.4	7.2	0.3
Samoa (14.4S,170.6W)	20.5	16.5	0.22	4.0	6.9	0.4
Fiji (18.1S,178.4E)	21.8	19.4	0.12	2.4	5.2	0.5
Site (2003-2007)	SCIA TTCO (DU)	SONDES TTCO (DU)	Relative difference	BIAS (DU)	RMS (DU)	R
Hilo (19.4N,155.4W)	26.1	28.2	0.08	-2.2	8.6	0.3
Paramaribo (5.8N,55.2W)	20.7	22.6	0.08	-1.8	5.4	0.5
Kuala Lumpur (2.7N,101.7E)	17.7	22.1	0.22	-4.4	6.9	0.5
Nairobi (1.3S,36.8E)	23.2	23.6	0.02	-0.4	5.4	0.2
Natal (5.4S,35.4W)	25.6	28.5	0.11	-2.9	7.8	0.5
Java (7.6S,111E)	18.0	22.2	0.21	-4.1	6.7	0.5
Ascension (8S,14.4W)	29.6	33.9	0.14	-4.3	7.9	0.5
Samoa (14.4S,170.6W)	18.4	16.0	0.14	2.4	8.1	0.3
Fiji (18.1S,178.4E)	21.8	20.7	0.05	1.2	5.7	0.6
Site (2008-2012)	GOME-2 TTCO (DU)	SONDES TTCO (DU)	Relative difference	BIAS (DU)	RMS (DU)	R
Hilo (19.4N,155.4W)	32.3	28.3	0.13	4.1	10.0	0.4
Paramaribo (5.8N,55.2W)	27.2	24.0	0.12	3.1	6.0	0.6
Kuala Lumpur (2.7N,101.7E)	21.3	21.6	0.02	-0.3	4.6	0.1
Nairobi (1.3S,36.8E)	27.9	24.5	0.13	3.4	4.8	0.3
Natal (5.4S,35.4W)	30.5	29.1	0.05	1.4	5.3	0.8
Java (7.6S,111E)	22.2	21.2	0.04	0.9	4.4	0.5
Ascension (8S,14.4W)	33.7	32.0	0.05	1.7	5.2	0.8
Samoa (14.4S,170.6W)	24.7	19.5	0.24	5.2	7.6	0.4
Fiji (18.1S,178.4E)	26.6	21.25	0.19	4.7	6.3	0.6

Table 6. Statistical comparison between CCD and LNM tropospheric ozone columns using SCIAMACHY data with ozonesondes for six SHADOZ sites. Information presented here: the ozonesonde site, the mean TTCO for CCD, LNM and for ozonesondes, the relative difference, the bias and the RMS difference between CCD TTCO and LNM TTCO and finally the correlation coefficient. The values are in DU.

Site (period: 2004-2011)	Mean CCD (DU)	Mean LNM (DU)	Mean Sondes (DU)	Relative difference CCD-LNM	Bias (DU)	RMS (DU)	R CCD VS Sondes	R LNM VS Sondes	R CCD VS LNM
Paramaribo (5.8N,55.2W)	26.9	29.8	23.2	0.10	-2.9	8.2	0.5	0.1	0.1
Kuala Lumpur (2.7N,101.7E)	18.1	18.5	21.7	0.02	-0.3	6.6	0.0	0.0	0.0
Nairobi (1.3S,36.8E)	26.8	21.5	24.2	0.22	5.3	7.6	0.2	0.3	0.2
Natal (5.4S,35.4W)	26.4	29.3	28.9	0.10	-2.9	6.1	0.7	0.6	0.5
Ascension (8S,14.4W)	30.6	30.0	33.1	0.02	0.7	4.5	0.5	0.6	0.4
Samoa (14.4S,170.6W)	18.4	20.0	18.0	0.08	-1.5	8.1	0.3	0.4	0.1
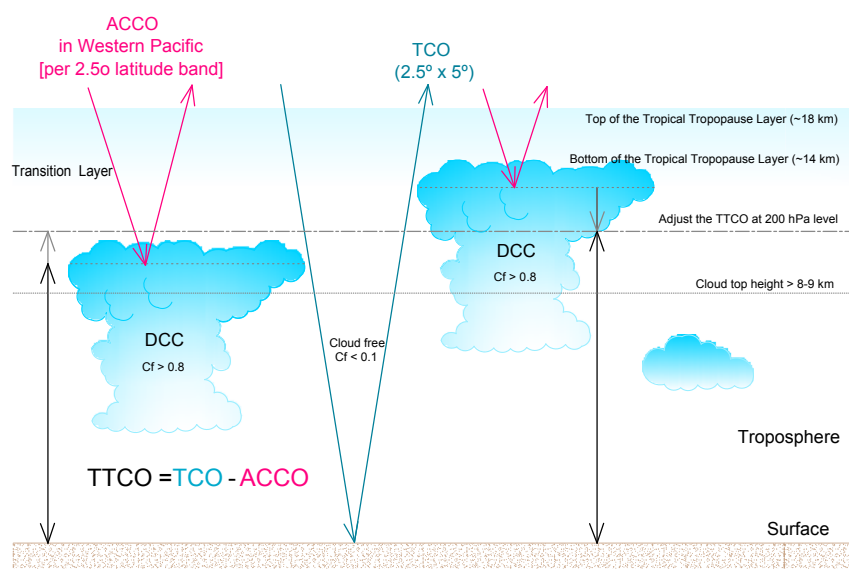
Figure 1. Illustration of the Convective Clouds Differential (CCD) technique. DCC are the deep convective cloud, cf is the cloud fraction, ACCO is the above cloud column of ozone, TCO is the total column of ozone and TTCO is the tropical tropospheric column of ozone.
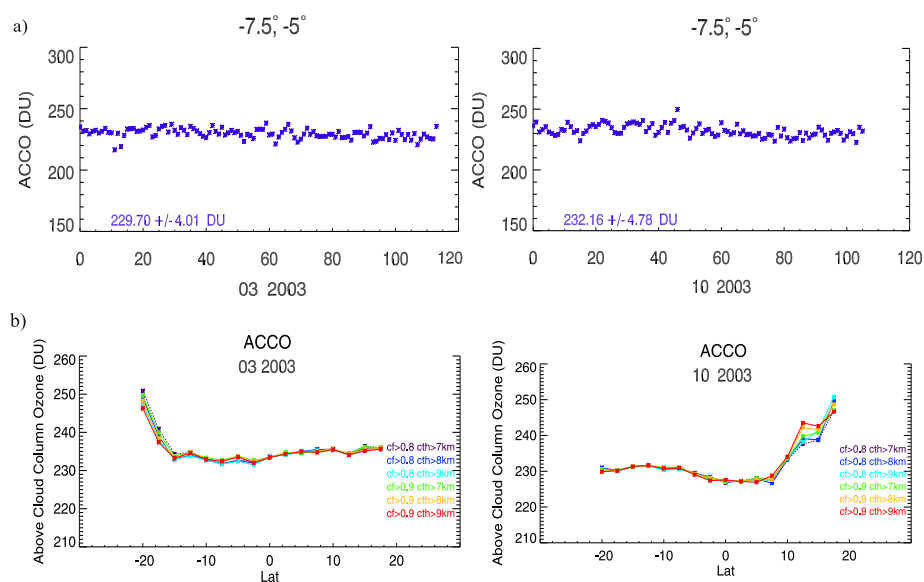
Figure 2. a) Above-cloud column ozone (ACCO), for the latitude band -7.5°S–5°S (cf>0.8 and cth >9 km) from SCIAMACHY (using OCRA/SACURA for cloud detection), in March and October 2003. The 1σ standard deviation is less than 5 DU. b) SCIAMACHY ACCO per 2.5° latitude bands in the Indian Ocean (70°E–170°W) for different cloud fractions (0.8, 0.9) and cloud top heights (7-9 km) in March and in October 2003.
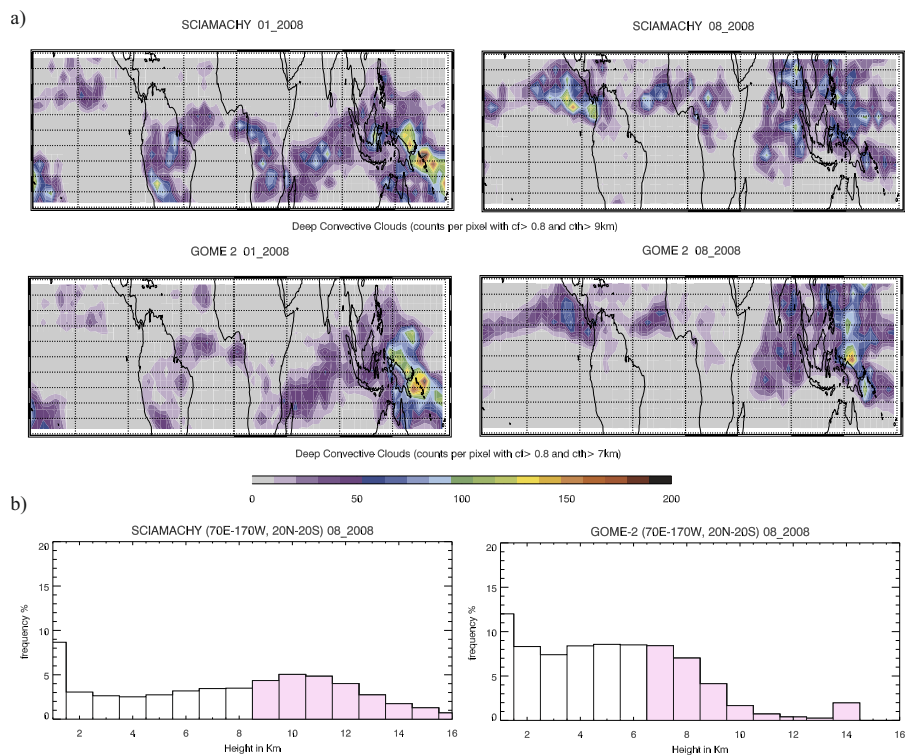
Figure 3. a) The number of counts per gridbox with cf greater than 0.8 and cth greater than 9 km (SCIA-MACHY) and cth greater than 7 km (GOME-2) for January and August 2008. b) Frequency of cloud top heights (cth) for August 2008 from SCIAMACHY (SACURA) and GOME-2 (ROCINN) in the Western Pacific area (20°S–20°N, 70°E–170°W)
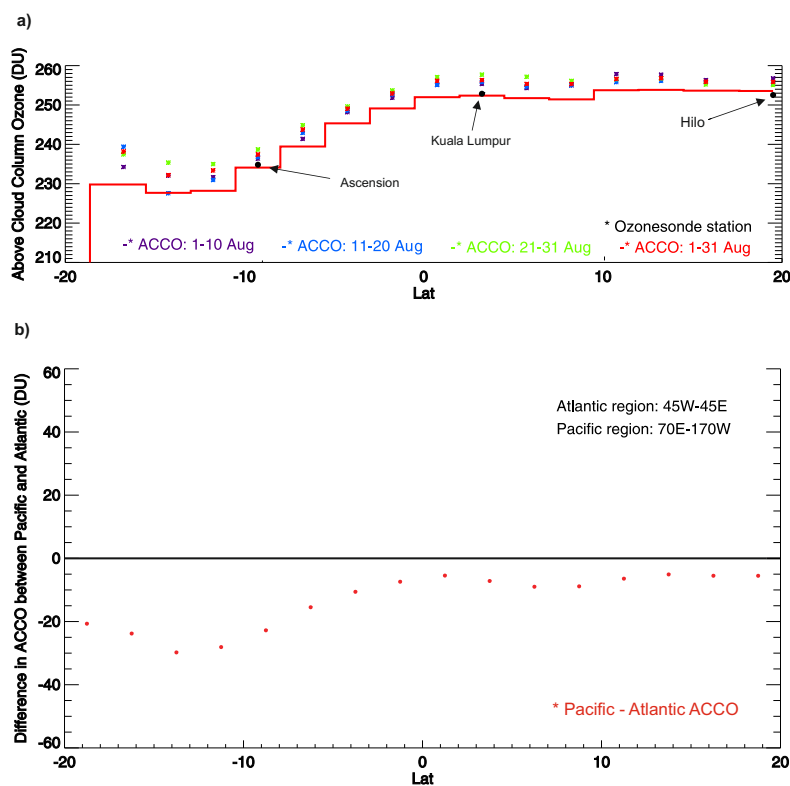
Figure 4. a) Above cloud column of ozone (ACCO) for August 2008, retrieved using 10 days time step (magenta, blue and green dots) and monthly averaged data (red dots) for 2.5° latitude bands from GOME-2 in August 2008. With red lines are plotted the final ACCO values, after the corrections applied for adjusting to the 200 hPa level and screening out the outlier data. With black dots are shown the stratospheric columns of ozone for the stations of Ascension, Kuala Lumpur and Hilo. b) The difference between the above cloud column calculated from the "reference" region in Western Pacific (70°E–170°W, 20°S–20°N) with the above cloud column calculated in Atlantic region (45°E–45°W, 20°S–20°N).
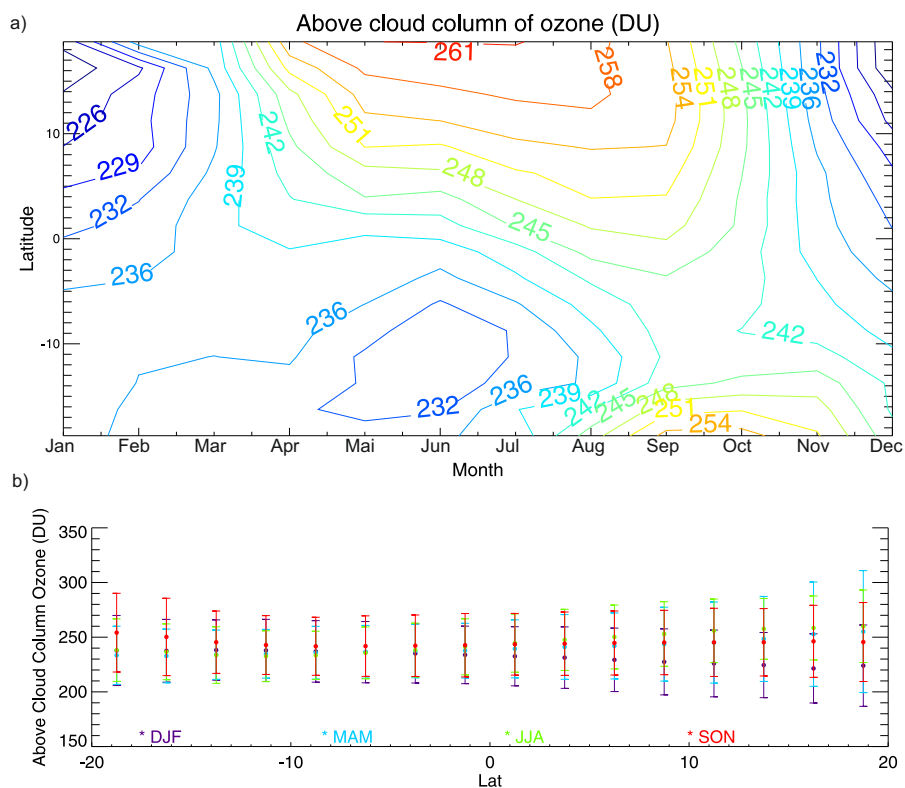
Figure 5. a) Zonal mean climatology of above-cloud column ozone (ACCO) in the Western Pacific region (20°S–20°N, 70°E–170°W) derived for the years 1996-2012 for 2.5° latitude bins. b) Scatter plot of seasonally averaged ACCO for the years 1996-2012. The error bars denote 1σ standard deviation.
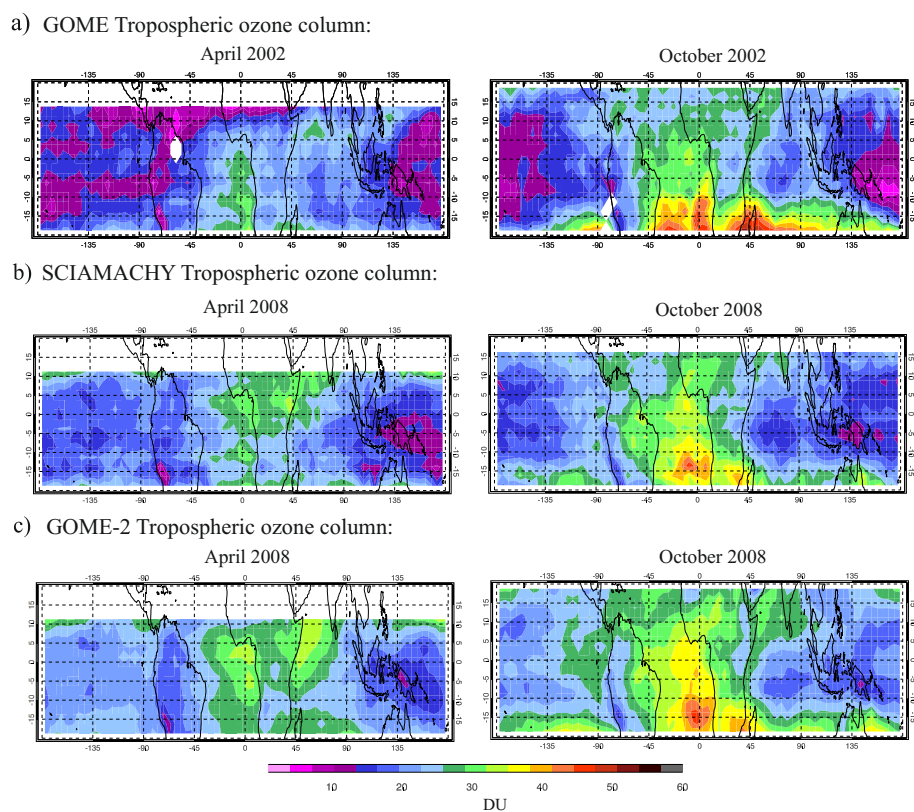
Figure 6. Tropical troposheric ozone column (TTCO) derived with the convective cloud differential (CCD) technique for April and October for a) GOME in 2002 for b) SCIAMACHY and c) GOME-2 both in 2008
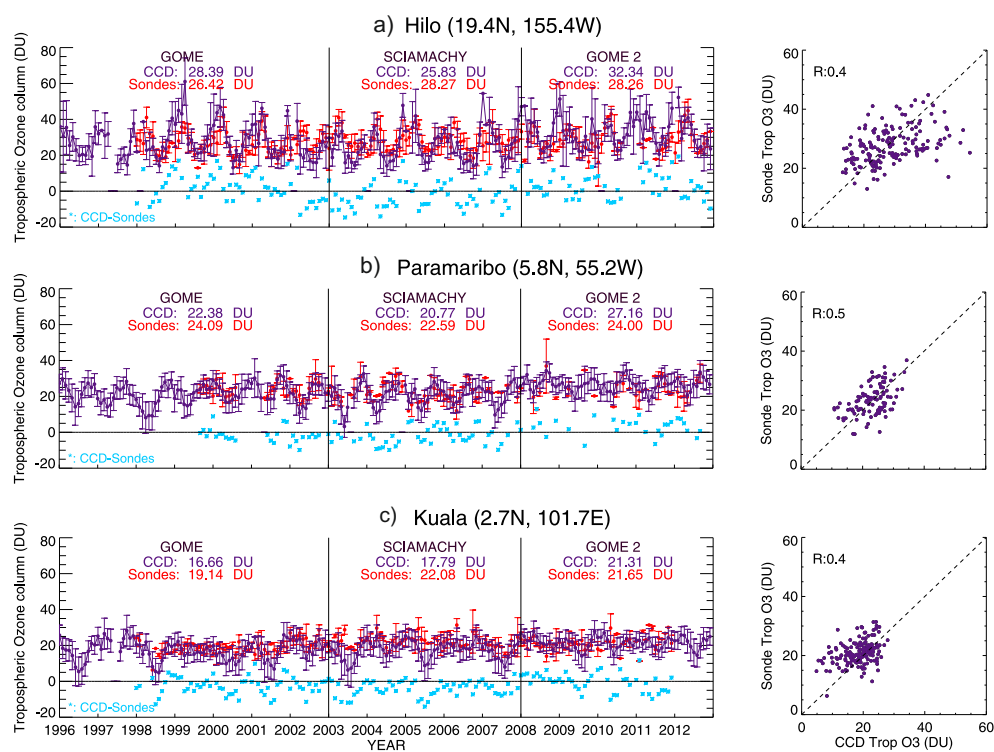
Figure 7. Time series of monthly mean CCD tropospheric ozone columns and collocated monthly mean SHADOZ ozonesonde TTCO in Hilo, Paramaribo, and Kuala Lumpur. The red lines give the integrated ozone column from integrating sonde ozone up to the fixed level of 200 hPa (roughly 12 km). The blue lines are: (i) GOME-1 CCD ozone columns (1996-2002), (ii) SCIAMACHY CCD ozone columns (2003-2007), and (iii) GOME-2 CCD ozone columns (2008-2012). Error bars indicate the standard deviation of the monthly mean. No error bars are shown for months with only one ozonesonde launch available. The difference between CCD and ozonesondes is plotted with light blue colour.
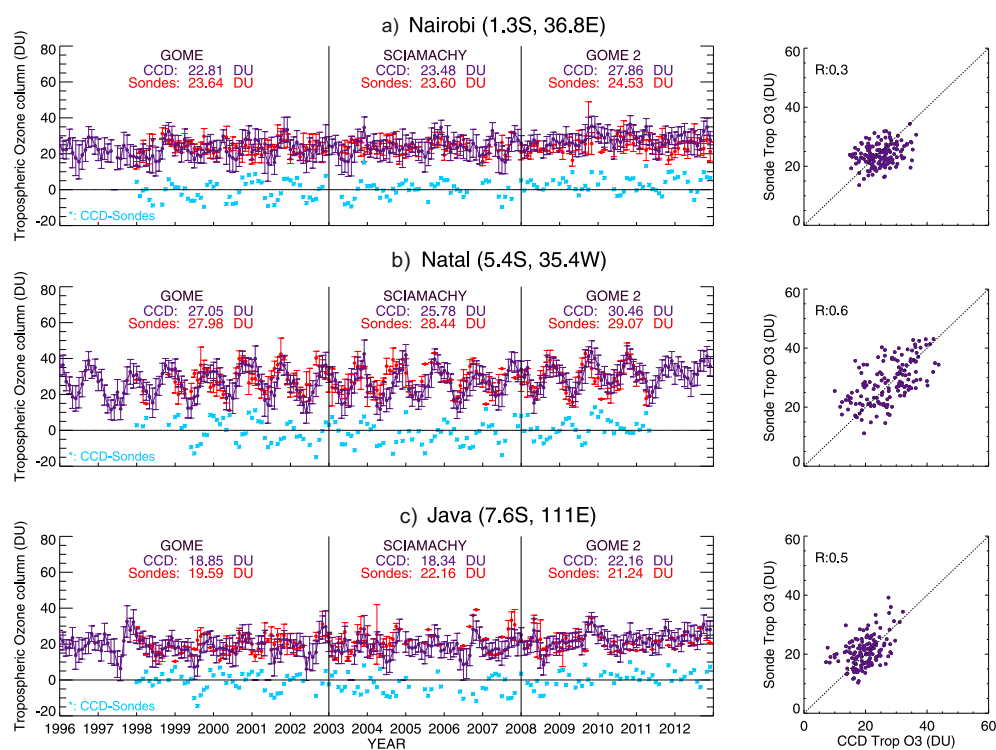
Figure 8. Time series of monthly mean CCD tropospheric ozone columns and collocated monthly mean SHADOZ ozonesonde TTCO in Nairobi, Natal, and Java. The red lines give the integrated ozone column from integrating sonde ozone up to the fixed level of 200 hPa (roughly 12 km). The blue lines are: (i) GOME-1 CCD ozone columns (1996-2002), (ii) SCIAMACHY CCD ozone columns (2003-2007), and (iii) GOME-2 CCD ozone columns (2008-2012). Error bars indicate the standard deviation of the monthly mean. No error bars are shown for months with only one ozonesonde launch available. The difference between CCD and ozonesondes is plotted with light blue colour.
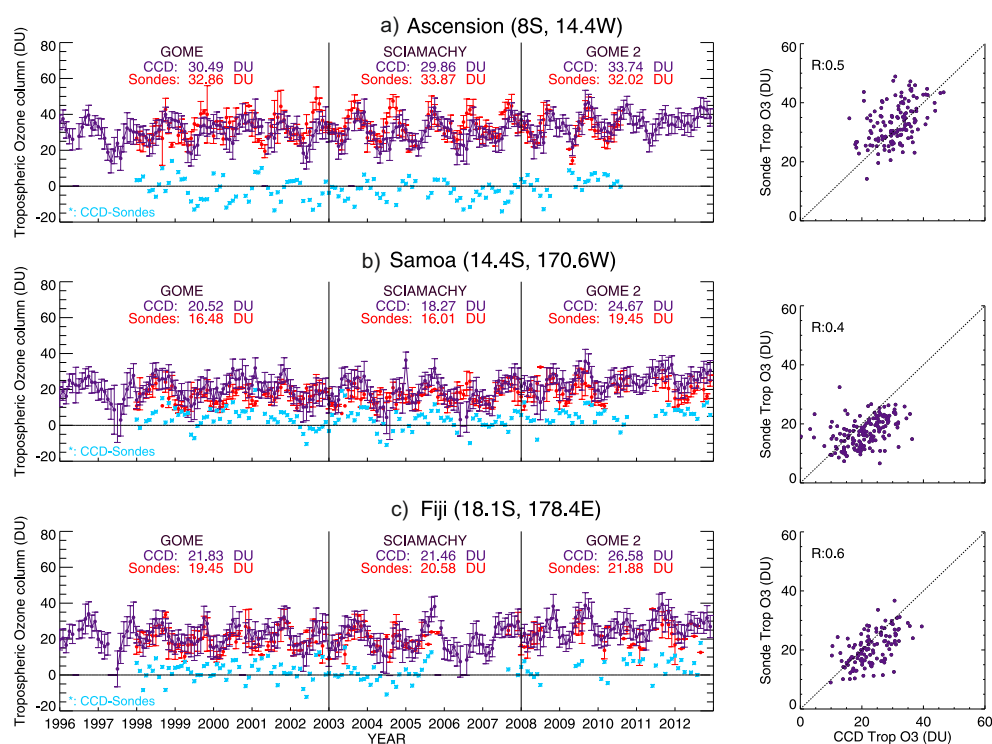
Figure 9. Time series of monthly mean CCD tropospheric ozone columns and collocated monthly mean SHADOZ ozonesonde TTCO in Ascension, Samoa, and Fiji. The red lines give the integrated ozone column from integrating sonde ozone up to the fixed level of 200 hPa (roughly 12 km). The blue lines are: (i) GOME-1 CCD ozone columns (1996-2002), (ii) SCIAMACHY CCD ozone columns (2003-2007), and (iii) GOME-2 CCD ozone columns (2008-2012). Error bars indicate the standard deviation of the monthly mean. No error bars are shown for months with only one ozonesonde launch available. The difference between CCD and ozonesondes is plotted with light blue colour.
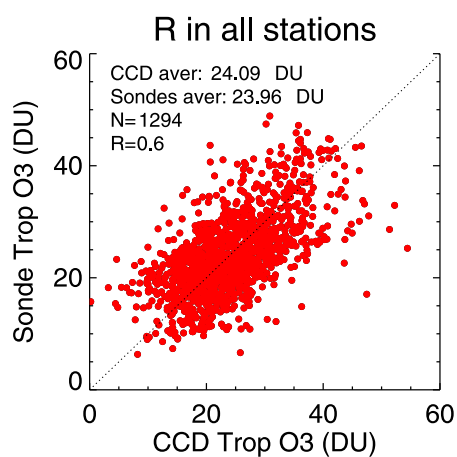
Figure 10. Correlation coefficient for all the ozonesonde stations and satellite instruments used for the comparison between 1996 and 2012.
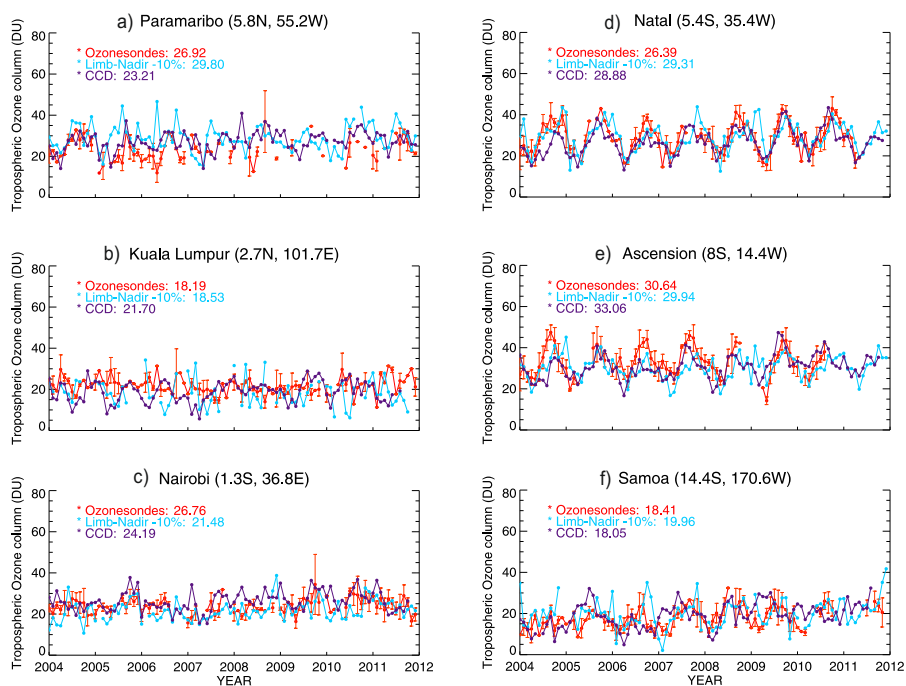
Figure 11. Timeseries of SCIAMACHY tropospheric ozone columns up to 200 hPa from LNM/ SCIAMACHY (blue), CCD (violet), and collocated sondes (red) from six SHADOZ stations.